

Hesperidin Targets *Leishmania donovani* Sterol C-24 Reductase to Fight against Leishmaniasis

Shams Tabrez, Fazlur Rahman, Rahat Ali, Sajjadul Kadir Akand, Mohammed A. Alaidarous, Saeed Banawas, Abdul Aziz Bin Dukhyil, and Abdur Rub*

Cite This: *ACS Omega* 2021, 6, 8112–8118

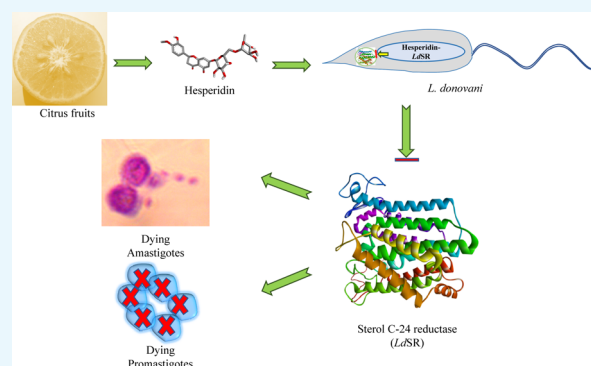
Read Online

ACCESS |

Metrics & More

Article Recommendations

ABSTRACT: Hesperidin, a naturally occurring flavanoid, is present in citrus family of fruits. It was found effective against an array of pathogens including fungi, bacteria, viruses, and protozoa. Here, we evaluated its antileishmanial activity and possible mechanism of action through different *in vitro* and *in silico* experiments. It inhibited the growth and proliferation of the parasites significantly with a IC₅₀ value of 1.019 ± 0.116 mM *in vitro*. It also reduced the growth of intramacrophagic amastigotes with a IC₅₀ value of 0.2858 ± 0.01398 mM. It induced the reactive oxygen species (ROS) in parasites in a dose-dependent manner. Through 2,7-dichloro dihydro fluorescein diacetate (H₂DCFDA) staining, it was observed that around 96.9% parasites were ROS positive at 2.0 mM concentration of hesperidin. The ROS generated led to the apoptosis of parasites in a dose-dependent manner as observed by annexin/PI staining. Molecular docking with one of the very important and unique drug-targets of *Leishmania donovani* sterol C-24 reductase resulted in its significant inhibition. Here, we for the first time showed that hesperidin induced the antileishmanial response through the induction of apoptosis and inhibition of sterol C-24 reductase. Our study will be helpful in the development of a cost-effective antileishmanial lead with higher efficacy.



1. INTRODUCTION

Leishmaniasis is a vector-borne disease caused by obligate intra-macrophage protozoa belonging to the genera *Leishmania*. The disease leishmaniasis is endemic in more than 89 different countries worldwide including Tropics, Subtropics, and Southern Europe. It is classified as a neglected tropical disease.¹ Worldwide, 0.7–1 million new cases of leishmaniasis are reported per year.² These days, paromomycin, amphotericin B, liposomal amphotericin, and miltefosine are the only available treatment of visceral leishmaniasis which have their own limitations due to high toxicity, resistance, and high cost.^{2,3} *Leishmania* exploits the host cholesterol biosynthetic machinery for its virulence, survival, and growth.^{4–6} *Leishmania* requires ergosterol for its membrane organization and other biological functions.⁷ Sterol C-24 reductase (*LdSR*), sterol alpha-14 demethylase, sterol 24-C-methyltransferase, and so forth are the major enzymes of the ergosterol biosynthetic pathway of *Leishmania donovani* which are still not studied in detail yet.⁷ Out of these, *LdSR* converts ergostatetraenol to ergosterol. It is an important drug-target for the development of new molecules to fight leishmaniasis.⁸ Hesperidin is a naturally occurring flavanone glycoside.⁹ It is present in high quantity in *Citrus aurantium*, *Citrus sinensis*, and *Citrus unshiu* and other species of this genus.^{10,11} It showed profound

antioxidant, anti-inflammatory, anti-proliferative, and anti-cancer activities.¹² The available literature reported that hesperidin inhibited the growth of different types of microbes including fungi, bacteria, virus, protozoa, and so forth.^{13–15} Anti-fungal effects of hesperidin are well-documented on different fungal species including *Aspergillus parasiticus*, *Aspergillus flavus*, *Fusarium semitectum*, and *Penicillium expansum*. Hesperidin detoxifies the effects of patulin, a mycotoxin released from *Aspergillus* also.¹⁶ Novel herbal micro-emulsion of hesperidin was found effective against bacterial species including *Escherichia coli*, *Staphylococcus epidermidis*, *Bacillus cereus*, *Enterococcus faecalis*, *Salmonella typhimurium*, *Klebsiella pneumoniae*, and *Pseudomonas aeruginosa*. Hesperidin pre-treatment suppressed infection-induced endotoxic shock in mice and reduced bacterial colonies during infection.^{17,18} Besides the anti-fungal and anti-bacterial role, the anti-viral effects of hesperidin are well established against

Received: December 2, 2020

Accepted: March 9, 2021

Published: March 16, 2021



HIV and herpes simplex virus type 2.¹⁹ Recently, hesperidin was shown to inhibit SARS-CoV-2 main protease and angiotensin-converting enzyme 2 receptor.^{20,21} In case of humans, hesperidin appeared to be safe with no adverse effects as reported in the treatment of hyperuricemia.⁹

Keeping all these medicinal values of hesperidin in mind, we planned to evaluate its antileishmanial activity on *L. donovani*. We have also performed the molecular docking of hesperidin against an important drug-target *LdSR* to dissect the possible mechanism of action of it. The current work may open new possibilities for the development of effective treatment against leishmaniasis.

2. RESULTS AND DISCUSSION

2.1. Antileishmanial Activity of Hesperidin. Logarithmic phase promastigote was treated with different concentrations of hesperidin. After 24 h of treatment, it inhibited the growth of parasite significantly. The IC_{50} value was calculated as 1.019 ± 0.116 mM (Figure 1A) by the dose response curve.

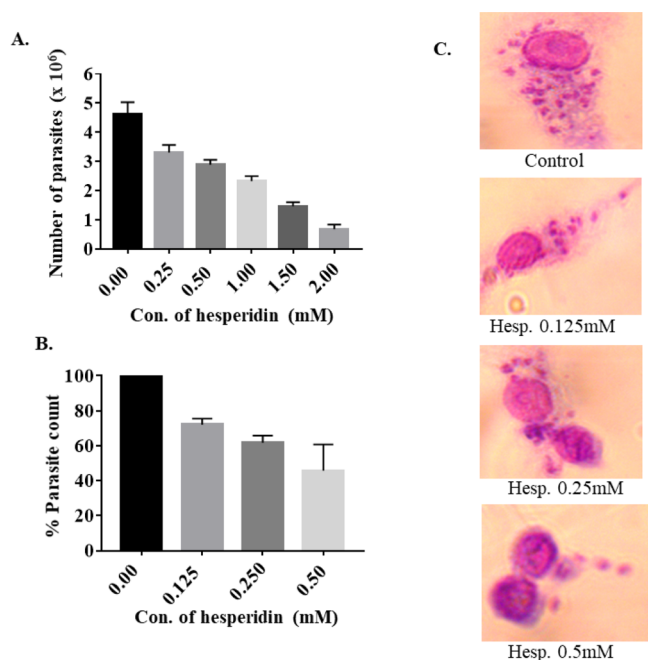


Figure 1. Antileishmanial evaluation of hesperidin. (A) Logarithmic phase, *L. donovani* promastigotes (2×10^6 parasites/mL) were treated with increasing concentration of hesperidin for 24 h, and the number of promastigotes were counted to determine IC_{50} value. (B) THP-1-derived macrophages were infected with *L. donovani* for 48 h and treated with hesperidin for 24 h post-infection. Finally, slides were fixed, stained, and dried, and % amastigotes were counted and IC_{50} value was determined. (C) Micrographs of THP-1-derived macrophages infected with *L. donovani* upon hesperidin treatment. Each point or bar corresponds to the mean \pm standard error.

The infective stage, promastigote that grows in the gut of sandfly, is transmitted to humans through the bite of sandflies. Macrophages phagocytose the promastigotes, where it gets transformed into an amastigote form. These amastigotes multiply within the macrophages and eventually propagate inside the body. Any drug-molecule must inhibit the growth of these intracellular amastigotes to be proven as an effective antileishmanial lead. Therefore, the differentiated macrophages were infected by *L. donovani* and treated with hesperidin. The

IC_{50} of the hesperidin on intra-macrophagic parasites was determined as 0.2858 ± 0.01398 mM (Figure 1B). A dose-dependent inhibition of the intra-macrophagic parasite was observed in microscopic images (Figure 1C).

2.2. Estimation of Hesperidin-Induced ROS. Reactive oxygen species (ROS) is the signal of stress and an important mediator of cell death and necrosis. We planned to check whether hesperidin-induced inhibition of parasite growth is related to the induction of apoptosis. To study this, hesperidin-treated parasites were stained with H_2DCFDA dye and analyzed through a flow cytometer. H_2DCFDA fluoresces upon the generation of OH^\bullet radicals and H_2O_2 . The fluorescence intensity is directly proportional to ROS generation, and the peak intensity was shifted to the right with increasing intensity. Hesperidin induced ROS generation in a dose-dependent manner in parasites (Figure 2A). It induced ROS in around 96.9% parasites at 2.0 mM concentration (Figure 2A).

2.3. Hesperidin Induced Apoptosis-Like Cell Death in *L. donovani*. Higher levels of ROS generally induce apoptosis in particular cells. Therefore, we further performed the annexin V/PI staining to check whether hesperidin-induced ROS ultimately induced the apoptosis-like cell death process in parasites. We observed a dose-dependent increase in a number of parasites undergoing apoptosis upon treatment of hesperidin. There were 96.9% parasites that have undergone apoptosis-like cell death at 2.0 mM concentration of hesperidin (Figure 2B). These results suggested that hesperidin induced ROS which ultimately led to the apoptosis-like cell death in parasites *in vitro*.

2.4. Homology Modelling and Molecular Docking of Hesperidin with *LdSR*. *LdSR* is one of the key enzymes of the ergosterol biosynthetic pathway which converts ergostatrienol to ergosterol. It is an attractive drug-target for the identification of new drug against leishmaniasis.⁸ We planned to perform the molecular docking of hesperidin against *LdSR* to investigate the possible mechanism of action. Hundred models of *LdSR* were generated and best one was selected based on the lowest dope score (Figure 3A–D). Three-dimensional (3D) cartoon, Ramachandran plot, and structural topologies of the generated model of *LdSR* were prepared for further molecular docking studies (Figure 3A–D). It showed the lowest binding energy of -10.1 kcal/mol and highest affinity toward hesperidin (Table 1). The binding pattern of hesperidin with *LdSR* depicts the loss of substrate accessibility and its inhibition (Figure 4A). Hesperidin interacts with Cys304(3), Thr307, and Arg464(2) binding site residues of *LdSR* by forming six intermolecular hydrogen bonds (Figure 4B,C). The bond length of hydrogen bonds was between 2.38 and 3.08 Å. One of the carbon ring of hesperidin formed π -anion bond with Asp468 of *LdSR* to stabilize the interaction (Figure 4B,C). The π -anion is recognized as an important noncovalent interaction in the biological structure, driven by polarization and electrostatic effects.²² Phe416 forms the π - π T-shaped as well as carbon hydrogen bond with the aromatic ring of hesperidin. This interaction plays an important role in the macromolecular structure and function.²³ The minimum binding energy and predicted inhibitory constant of hesperidin with respect to *LdSR* were calculated as -10.1 kcal/mol and 7.43 μ M, respectively (Table 1). This value of inhibitory constant suggested the effective inhibition of *LdSR* and possible leishmanicidal activity of hesperidin.

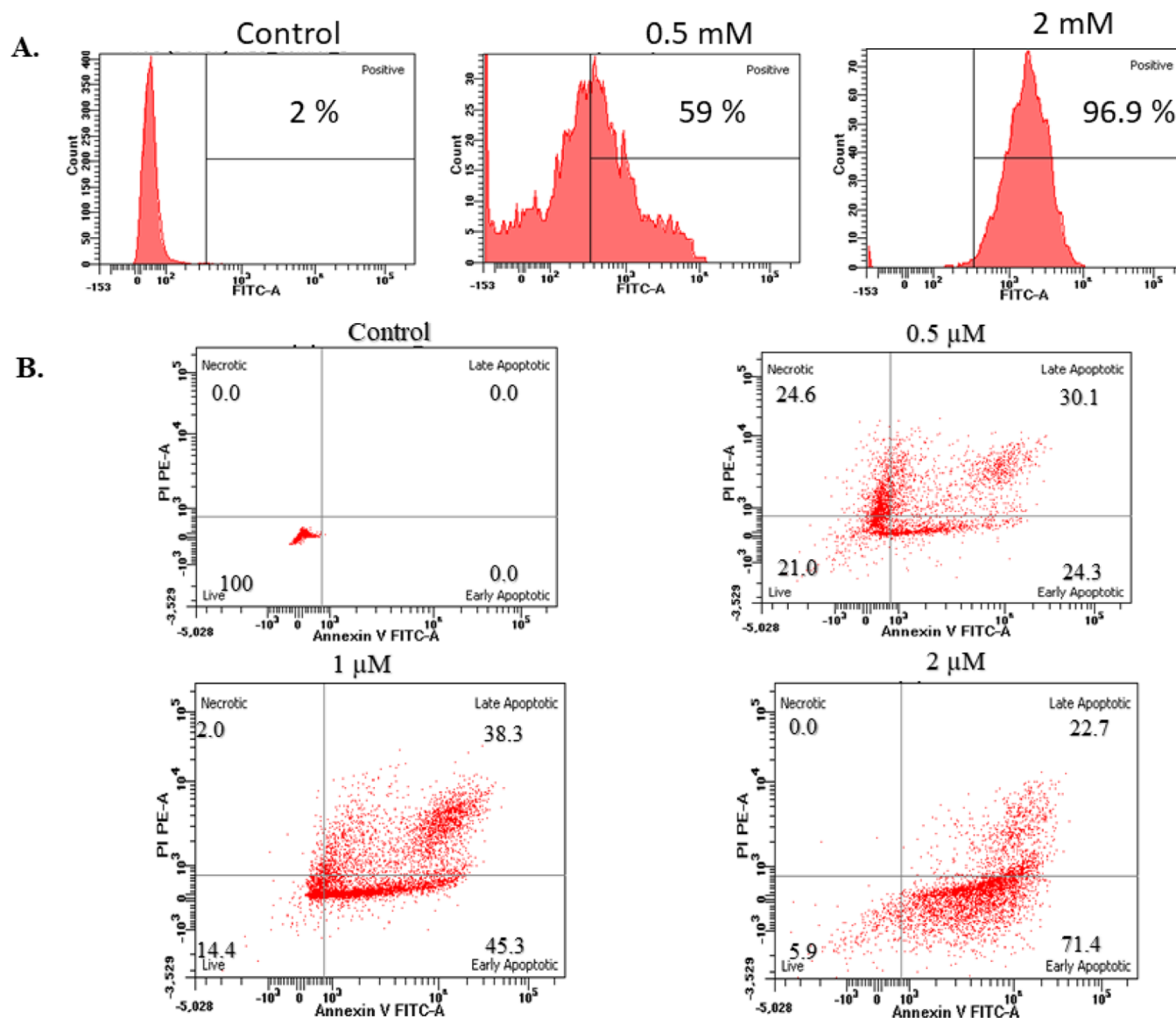


Figure 2. Hesperidin-induced ROS and apoptosis in parasites (A) 2×10^6 parasites/mL were incubated with low and high doses of hesperidin for 24 h followed by staining with H_2DCFDA dye for ROS analysis through a flow cytometer (B). Parasites were incubated with different concentrations of hesperidin for 24 h, followed by staining with annexin V-FITC/PI to assess the apoptosis through a flow cytometer as described in methods.

Overall, our study suggested the antileishmanial activity of hesperidin with ROS generation and apoptosis-like cell death induction in parasites along with the possible inhibition of a key ergosterol-biosynthetic enzyme, *LdSR*. In addition to this the generated results could not rule out the other possible targets of hesperidin in *L. donovani* that might be contributing in its antileishmanial response.

3. MATERIALS AND METHODS

3.1. Parasite and Cell Culturing. *L. donovani* cultures (MHOM/IN/83/AG83) were maintained in M199 media pH 7.4, supplemented with 10% heat-inactivated fetal bovine serum (FBS), and 1% penicillin–streptomycin antibiotic at 24 °C. The logarithmic phase parasites were regularly passaged at 3–4 days at the density of 2×10^6 parasites/mL. THP-1 cell line (human leukemia cells) was cultured in RPMI-1640 media with 10% FBS and 1% penicillin–streptomycin antibiotic and maintained at 37 °C and 5% CO_2 . The stock concentration of

the compound was prepared in blank M199 media. THP-1 monocytic cells were stimulated with 20 ng/mL of phorbol myristate acetate for differentiation to macrophages.

3.2. Antileishmanial Activity of Hesperidin. For antileishmanial activity, logarithmic phase parasites were seeded at the density of 2×10^6 parasites/mL in complete M199 media; then, the compounds were added at different concentrations. After 24 h of incubation at 24 °C, the parasites were fixed in 1% paraformaldehyde and enumerated using a hemocytometer. The percentage inhibition was calculated, by considering negative control as 100%. Dose–response curves were plotted using inhibitor concentration versus normalized response and IC_{50} calculated automatically²⁴

3.3. Parasite Load Calculation in Macrophages. For amastigote assay, 2×10^5 THP-1 cells were seeded on the coverslip in a six-well plate, and the differentiated macrophages were infected with log-phase virulent promastigotes in the ratio of 1:10 (macrophage: *Leishmania*) for 24 h. The non-

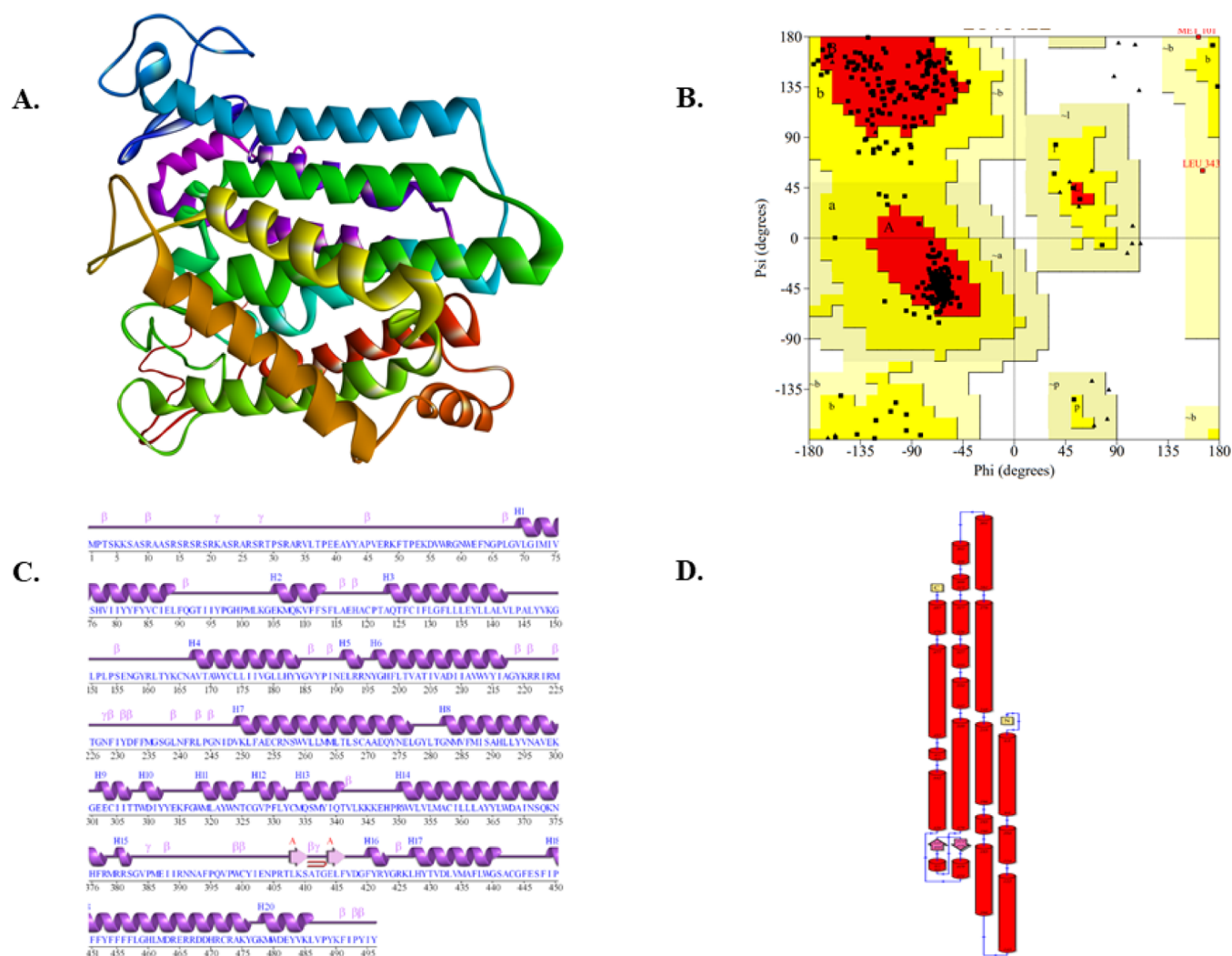


Figure 3. Homology modelling and validation of *LdSR*. (A) Three-dimensional cartoon representation of sterol C-24 reductase. (B) Ramachandran plot by RAMPAGE: Ramachandran plot showed 100% residues in the allowed region. (C) Secondary structure elements and (D) topology map of sterol C-24 reductase, indicating a conserved α and β framework.

Table 1. Molecular Docking Interaction of Hesperidin with *LdSR*^a

s. no.	proteins	binding energy (kcal/mol)	pK_i^{pred} (μM)	interacting Residues	no. of H-bonds
1	Sterol C-24 reductase	-10.1	7.43	Tyr294, Cys304, Ile305, Thr307 , Thr308, Trp367, Lys374, Phe377, Arg378, Leu415, Phe416, Val417, Tyr421, His428, Tyr429, Asp432, Phe457, Leu461, Arg464 , Asp468, Arg471, Cys472, Tyr476, Trp480, Tyr483	6

^aAbbreviations: pK_i —negative decimal logarithm of inhibition constant; pred—predicted. Bold letters: represent residues forming hydrogen bonds.

phagocytosed parasites were washed, and infected macrophages were treated with different doses of hesperidin for 24 h post-infection. The coverslip was washed with 1× phosphate-buffered saline (PBS), fixed with chilled methanol, and stained using modified Giemsa stain for amastigote microscopic evaluation. About 100 macrophages were counted from different focus to evaluate the effect of the treatment on the intra-macrophagic parasite burden²⁵

3.4. Estimation of ROS Generation. To estimate the effects of hesperidin on ROS generation, 2,7-dichloro dihydro fluorescein diacetate (H₂DCFDA) dye was used. The treated parasites were washed with PBS and incubated with 10 μM of H₂DCFDA for 20 min in dark. The fluorescent signal of each

sample was acquired using a BD FACS ARIA III flow cytometer, and the recorded data was represented in the form of histograms.

3.5. Apoptotic Assay. For the apoptotic assay, treated and untreated parasites were centrifuged at 3000g for 5 min and washed thrice with 1× PBS. Finally, the pellet was resuspended in 1× binding buffer (10 mM Hepes pH 7.4, 140 mM NaCl and 2.5 mM CaCl₂) containing 5 μL of annexin-FITC and 5 μL of propidium iodide for 25 min in dark at room temperature. The samples were analyzed through a BD FACSAria III Cell Sorter.

3.6. Molecular Docking, Homology Modelling, Receptor, and Ligand Preparations. PyRx was used for the

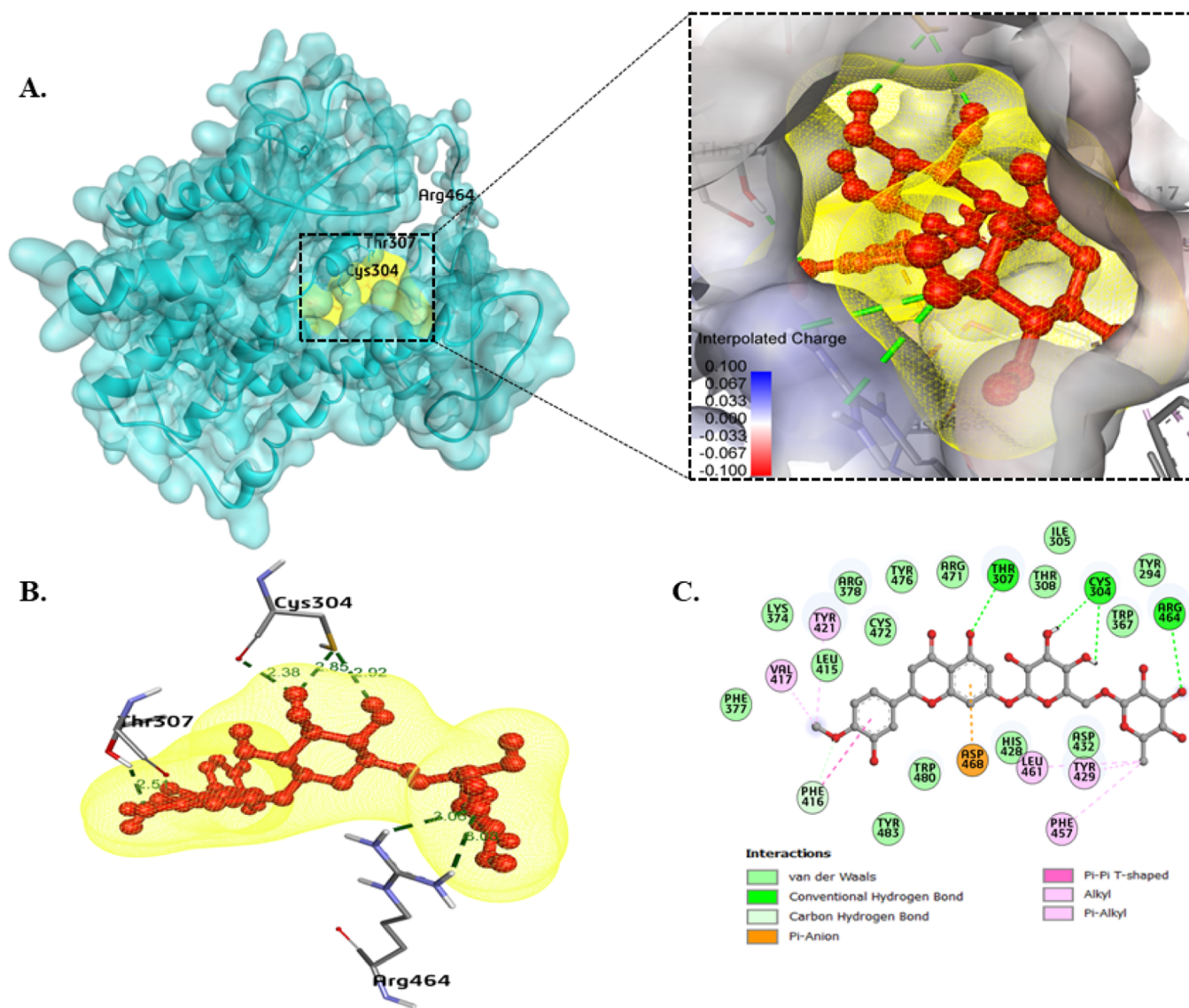


Figure 4. *In silico* analysis of the binding pattern of hesperidin with *L. donovani* LdSR: (A) Cartoon-surface representation of LdSR with hesperidin (red ball and stick with a yellow surface meshwork) after docking. (B) Significant interactions were observed with functionally important residues of LdSR. (C) 2D plot of interaction of LdSR with hesperidin.

virtual screening of the ligand with the target proteins of *L. donovani*.^{26,27} The detailed interactions and their types including hydrogen bonds, van der Waals interactions, alkyl, π -alkyl, halogen, and so forth were analyzed by BIOVIA Discovery Studio.²⁸ The most favorable binding poses of the compounds were analyzed by choosing the lowest free energy of binding (ΔG) and the lowest inhibition constant (K_i) which is calculated using the following formula

$$K_{i\text{pred}} = \text{exponential}^{\Delta G/RT}$$

where ΔG is binding affinity (kcal/mol), R (gas constant) is $1.98 \text{ cal K}^{-1} \text{ mol}^{-1}$, and T (room temperature) is 298.15 K.

The protein sequence of LdSR (CBZ37214.1) enzyme of *L. donovani* was retrieved from NCBI. For the identification of similar templates, blastP²⁹ was performed against Protein Data Bank. The X-ray diffracted crystal structure 2.74 Å resolution (PDB id: 4QUV_A) was used as a template structure to model the 3D structure of sterol C-24 reductase. Modeller 9.24³⁰ was used for homology modelling, and the generated model was

assessed by the PROCHECK program and PDB sum tool, and Ramachandran plots were also generated.^{31,32} The critical residues of the binding pocket was identified from the native catalytic pockets of the available crystal structure of proteins, CASTp, and Discovery studio. The 3D structure of hesperidin was retrieved from PubChem database.³³ The atomic coordinates of the hesperidin was changed to pdbqt set-up using Open Babel GUI,³⁴ and Universal Force Field (uff) was used for the energy minimization.³⁵

3.7. Statistical Analysis. All the experiments were performed in triplicate, and the results represented are the mean of the triplicate with SD. Statistical analysis was performed using Graph pad prism 7.0 software, and a P -value of less than 0.05 was considered significant. The statistical significance was calculated using one way ANOVA followed by Dunnett's multiple comparison test.

4. CONCLUSIONS

It is the first and preliminary study on the evaluation of antileishmanial potential of hesperidin. Further, our study will

provide a platform for the future detailed *in vitro* and *in vivo* study in this context for the possible use of hesperidin in the treatment of visceral leishmaniasis.

AUTHOR INFORMATION

Corresponding Author

Abdur Rub – Infection and Immunity Laboratory (414), Department of Biotechnology, Jamia Millia Islamia (A Central University), New Delhi 110025, India; orcid.org/0000-0003-1301-0761; Phone: +91-9560887383; Email: arub@jmi.ac.in

Authors

Shams Tabrez – Infection and Immunity Laboratory (414), Department of Biotechnology, Jamia Millia Islamia (A Central University), New Delhi 110025, India

Fazlur Rahman – Infection and Immunity Laboratory (414), Department of Biotechnology, Jamia Millia Islamia (A Central University), New Delhi 110025, India

Rahat Ali – Infection and Immunity Laboratory (414), Department of Biotechnology, Jamia Millia Islamia (A Central University), New Delhi 110025, India

Sajjadul Kadir Akand – Infection and Immunity Laboratory (414), Department of Biotechnology, Jamia Millia Islamia (A Central University), New Delhi 110025, India

Mohammed A. Alaidarous – Department of Medical Laboratory Sciences, College of Applied Medical Sciences and Health and Basic Sciences Research Center, Majmaah University, Al Majmaah 11952, Saudi Arabia

Saeed Banawas – Department of Medical Laboratory Sciences, College of Applied Medical Sciences and Health and Basic Sciences Research Center, Majmaah University, Al Majmaah 11952, Saudi Arabia; Department of Biomedical Sciences, Oregon State University, Corvallis, Oregon 97331, United States

Abdul Aziz Bin Dukhyil – Department of Medical Laboratory Sciences, College of Applied Medical Sciences and Health and Basic Sciences Research Center, Majmaah University, Al Majmaah 11952, Saudi Arabia

Complete contact information is available at:

<https://pubs.acs.org/10.1021/acsomega.0c05858>

Funding

The authors would like to thank the Deanship of Scientific Research at Majmaah University, Al Majmaah, 11952, Saudi Arabia for supporting this work under the group project number RGP-2019-31.

Notes

The authors declare no competing financial interest.

ACKNOWLEDGMENTS

The authors are thankful to the Central Instrumentation facility, Jamia Millia Islamia for support.

REFERENCES

- (1) Piscopo, T. V.; Mallia Azzopardi, C. Leishmaniasis. *Postgrad. Med. J.* **2007**, *83*, 649–657.
- (2) Burza, S.; Croft, S. L.; Boelaert, M. Leishmaniasis. *Lancet* **2018**, *392*, 951–970.
- (3) Searo, W. *Regional Strategic Framework for Elimination of Kala-azar from South-East Asia region (2005–2015)*; World Health Organization, Regional Office for South-East Asia: New Delhi, India, 2005, http://apps.who.int/pds_docs/B0211.pdf.
- (4) Yao, C.; Wilson, M. E. Dynamics of sterol synthesis during development of *Leishmania* spp. parasites to their virulent form. *Parasites Vectors* **2016**, *9*, 200.
- (5) Rub, A.; Dey, R.; Jadhav, M.; Kamat, R.; Chakkaramakkil, S.; Majumdar, S.; Mukhopadhyaya, R.; Saha, B. Cholesterol depletion associated with *Leishmania* major infection alters macrophage CD40 signalosome composition and effector function. *Nat. Immunol.* **2009**, *10*, 273–280.
- (6) Semini, G.; Paape, D.; Paterou, A.; Schroeder, J.; Barrios-Llerena, M.; Aebischer, T. Changes to cholesterol trafficking in macrophages by *Leishmania* parasites infection. *MicrobiologyOpen* **2017**, *6*, No. e00469.
- (7) de Souza, W.; Rodrigues, J. C. Sterol Biosynthesis Pathway as Target for Anti-trypanosomatid Drugs. *Interdiscip. Perspect. Infect. Dis.* **2009**, *2009*, 642502.
- (8) Urbina, J. A. Lipid biosynthesis pathways as chemotherapeutic targets in kinetoplastid parasites. *Parasitology* **1997**, *114*, S91–S99.
- (9) Garg, A.; Garg, S.; Zaneveld, L. J. D.; Singla, A. K. Chemistry and pharmacology of the Citrus bioflavonoid hesperidin. *Phytother. Res.* **2001**, *15*, 655–669.
- (10) Kaness, K.; Tisserat, B.; Berhow, M.; Vandercook, C. Phenolic composition of various tissues of rutaceae species. *Phytochemistry* **1993**, *32*, 967–974.
- (11) Kawaguchi, K.; Mizuno, T.; Aida, K.; Uchino, K. Hesperidin as an inhibitor of lipases from porcine pancreas and *Pseudomonas*. *Biosci. Biotechnol. Biochem.* **1997**, *61*, 102–104.
- (12) Sezer, A.; Usta, Z.; Usta, U.; Yagci, M. The effect of a flavonoid fractions diosmin + hesperidin on radiation-induced acute proctitis in a rat model. *J. Canc. Res. Therapeut.* **2011**, *7*, 152–156.
- (13) Abuelsaad, A. S. A.; Mohamed, I.; Allam, G.; Al-Solumani, A. A. Antimicrobial and immunomodulating activities of hesperidin and ellagic acid against diarrheic *Aeromonas hydrophila* in a murine model. *Life Sci.* **2013**, *93*, 714–722.
- (14) Parvez, M. K.; Tabish Rehman, M.; Alam, P.; Al-Dosari, M. S.; Alqasoumi, S. I.; Alajmi, M. F. Plant-derived antiviral drugs as novel hepatitis B virus inhibitors: Cell culture and molecular docking study. *Saudi Pharm. J.* **2019**, *27*, 389–400.
- (15) Allam, G.; Abuelsaad, A. S. A. In vitro and in vivo effects of hesperidin treatment on adult worms of *Schistosoma mansoni*. *J. Helminthol.* **2014**, *88*, 362–370.
- (16) Salas, M. P.; Céliz, G.; Geronazzo, H.; Daz, M.; Resnik, S. L. Antifungal activity of natural and enzymatically-modified flavonoids isolated from citrus species. *Food Chem.* **2011**, *124*, 1411–1415.
- (17) Karayıldırım, Ç. K. Characterization and in vitro Evolution of Antibacterial Efficacy of Novel Hesperidin Microemulsion. *Celal Bayar Üniv. Fen Bilim. Derg.* **2017**, *13*, 943–947.
- (18) Kawaguchi, K.; Kikuchi, S.-i.; Hasunuma, R.; Maruyama, H.; Yoshikawa, T.; Kumazawa, Y. A Citrus Flavonoid Hesperidin Suppresses Infection-Induced Endotoxin Shock in Mice. *Biol. Pharm. Bull.* **2004**, *27*, 679–683.
- (19) Garg, A.; Anderson, R. A.; Zaneveld, L. J.; Garg, S. Biological activity assessment of a novel contraceptive antimicrobial agent. *J. Androl.* **2005**, *26*, 414–421.
- (20) Das, S.; Sarmah, S.; Lyndem, S.; Singha Roy, A. An investigation into the identification of potential inhibitors of SARS-CoV-2 main protease using molecular docking study. *J. Biomol. Struct. Dyn.* **2020**, 1–11.
- (21) Joshi, R. S.; Jagdale, S. S.; Bansode, S. B.; Shankar, S. S.; Tellis, M. B.; Pandya, V. K.; Chugh, A.; Giri, A. P.; Kulkarni, M. J. Discovery of potential multi-target-directed ligands by targeting host-specific SARS-CoV-2 structurally conserved main protease. *J. Biomol. Struct. Dyn.* **2020**, 1–16.
- (22) Anstötter, C. S.; Rogers, J. P.; Verlet, J. R. R. Spectroscopic Determination of an Anion- π Bond Strength. *J. Am. Chem. Soc.* **2019**, *141*, 6132–6135.
- (23) Horowitz, S.; Triebel, R. C. Carbon-oxygen hydrogen bonding in biological structure and function. *J. Biol. Chem.* **2012**, *287*, 41576–41582.

(24) Tabrez, S.; Rahman, F.; Ali, R.; Alouffi, A. S.; Akand, S. K.; Alshehri, B. M.; Alshammari, F. A.; Alam, A.; Alaidarous, M. A.; Banawas, S.; Dukhyil, A. A. B.; Rub, A. Cynaroside inhibits *Leishmania donovani* UDP-galactopyranose mutase and induces reactive oxygen species to exert antileishmanial response. *Biosci. Rep.* **2021**, *41*, BSR20203857.

(25) Lima Asgharpour, S.; Parvaneh, R.-M.; Fatemeh, T.; Khadijeh, K. Evaluating the Effect of Cinnarizine on Promastigotes and Amastigotes forms of *Leishmania major*. *Infect. Disord.—Drug Targets* **2020**, *20*, 550–555.

(26) Dallakyan, S.; Olson, A. J. Small-molecule library screening by docking with PyRx. *Methods Mol. Biol.* **2015**, *1263*, 243–250.

(27) Bhowmik, S.; Akhter, S. A Computational Molecular Docking Studies on the Tryparedoxin Peroxidase of *Leishmania Donovani* Responsible for Visceral Leishmaniasis in Human. *Letts. Drug Des. Discovery* **2020**, *17*, 1–13.

(28) Shamsi, A.; Mohammad, T.; Anwar, S.; AlAjmi, M. F.; Hussain, A.; Rehman, M. T.; Islam, A.; Hassan, M. I. Glecaprevir and Maraviroc are high-affinity inhibitors of SARS-CoV-2 main protease: possible implication in COVID-19 therapy. *Biosci. Rep.* **2020**, *40*, BSR20201256.

(29) Mohammad, K.; Partha, P. M.; Yusuf, A.; Mohammed, A.; Abdur, R. Screening of Novel Inhibitors Against *Leishmania donovani* Calcium ion Channel to Fight Leishmaniasis. *Infect. Disord.—Drug Targets* **2017**, *17*, 120–129.

(30) Sali, A.; Blundell, T. L. Comparative protein modelling by satisfaction of spatial restraints. *J. Mol. Biol.* **1993**, *234*, 779–815.

(31) Laskowski, R. A.; Rullmann, J. A.; MacArthur, M. W.; Kaptein, R.; Thornton, J. M. AQUA and PROCHECK-NMR: programs for checking the quality of protein structures solved by NMR. *J. Biomol. NMR* **1996**, *8*, 477–486.

(32) Laskowski, R. A. PDBsum new things. *Nucleic Acids Res.* **2009**, *37*, D355–D359.

(33) Kashif, M.; Tabrez, S.; Husein, A.; Arish, M.; Kalaiarasan, P.; Manna, P. P.; Subbarao, N.; Akhter, Y.; Rub, A. Identification of novel inhibitors against UDP-galactopyranose mutase to combat leishmaniasis. *J. Cell. Biochem.* **2018**, *119*, 2653–2665.

(34) O'Boyle, N. M.; Banck, M.; James, C. A.; Morley, C.; Vandermeersch, T.; Hutchison, G. R.; Open Babel. An open chemical toolbox. *J. Cheminf.* **2011**, *3*, 33.

(35) Rappé, A. K.; Casewit, C. J.; Colwell, K. S.; Goddard, W. A., III; Skiff, W. M. UFF, a full periodic table force field for molecular mechanics and molecular dynamics simulations. *J. Am. Chem. Soc.* **1992**, *114*, 10024–10035.